

# Journal of Biomedical Optics

[SPIEDigitalLibrary.org/jbo](http://SPIEDigitalLibrary.org/jbo)

## **Stamping surface-enhanced Raman spectroscopy for label-free, multiplexed, molecular sensing and imaging**

Ming Li  
Jing Lu  
Ji Qi  
Fusheng Zhao  
Jianbo Zeng  
Jorn Chi-Chung Yu  
Wei-Chuan Shih

# Stamping surface-enhanced Raman spectroscopy for label-free, multiplexed, molecular sensing and imaging

Ming Li,<sup>a,†</sup> Jing Lu,<sup>a,†</sup> Ji Qi,<sup>a</sup> Fusheng Zhao,<sup>a</sup> Jianbo Zeng,<sup>a</sup> Jorn Chi-Chung Yu,<sup>b</sup> and Wei-Chuan Shih<sup>a,\*</sup>

<sup>a</sup>University of Houston, Department of Electrical and Computer Engineering, 4800 Calhoun Road, Houston, Texas 77204

<sup>b</sup>Sam Houston State University, Forensic Science Program, 1003 Bowers Boulevard, Huntsville, Texas 77341

**Abstract.** We report stamping surface-enhanced Raman spectroscopy (S-SERS) for label-free, multiplexed, molecular sensing and large-area, high-resolution molecular imaging on a flexible, nonplasmonic surface without solution-phase molecule transfer. In this technique, a polydimethylsiloxane (PDMS) thin film and nanoporous gold disk SERS substrate play the roles as molecule carrier and Raman signal enhancer, respectively. After stamping the SERS substrate onto the PDMS film, SERS measurements can be directly taken from the “sandwiched” target molecules. The performance of S-SERS is evaluated by the detection of Rhodamine 6G, urea, and its mixture with acetaminophen, in a physiologically relevant concentration range, along with the corresponding SERS spectroscopic maps. S-SERS features simple sample preparation, low cost, and high reproducibility, which could lead to SERS-based sensing and imaging for point-of-care and forensics applications. © The Authors. Published by SPIE under a Creative Commons Attribution 3.0 Unported License. Distribution or reproduction of this work in whole or in part requires full attribution of the original publication, including its DOI. [DOI: 10.1117/1.JBO.19.5.050501]

Keywords: surface-enhanced Raman spectroscopy; nanoporous gold disk; polydimethylsiloxane stamping; label-free molecular sensing and imaging; solution-phase molecule transfer.

Paper 140163LR received Mar. 13, 2014; revised manuscript received Apr. 4, 2014; accepted for publication Apr. 8, 2014; published online May 7, 2014.

## 1 Introduction

Surface-enhanced Raman spectroscopy (SERS) is a spectroscopic technique where Raman scattering is boosted primarily by enhanced electric field due to localized surface plasmon resonance.<sup>1</sup> With advances in nanofabrication techniques, SERS has attracted great attention for label-free molecular sensing and imaging.<sup>2,3</sup> However, the practical use of SERS has often encountered a couple of inherent issues. The first one is regarding a molecule transfer step where target molecules need to be

within the close proximity of an SERS-active surface by either mixing with nanoparticles or coating onto surface-bound nanostructures. In other words, target molecules are required to be transferred from non-SERS-active surfaces to SERS-active ones, normally in the solution phase, which can be problematic due to issues such as surface affinity variability and uncertainty, competitive adsorption among different molecules, and contamination issues, causing irreproducible results and erroneous or biased interpretations. More importantly, if the spatial distribution of molecules on the surface prior to the transfer step is of importance, such information is completely lost. Practically, solution-phase processes are relatively more labor and time consuming and require a “wet” laboratory. Furthermore, SERS measurements are always restricted to molecules adsorbed on metals such as Ag, Au, and Cu.

To address the aforementioned issues, many approaches have been developed, and can be broadly classified into chemical and physical means. Chemical approaches employ functionalized surfaces to improve affinity and selectivity of target molecules. For example, Au nanoparticles were surface-modified by cystamine<sup>4</sup> and cysteine<sup>5</sup> for detecting perchlorate and trinitrotoluene, respectively. Physical approaches, in contrast, attempt to bring the target molecules to the SERS-active surface by physical manipulation. A potential advantage of physical approach lies in that the SERS enhancement depends solely on distance, rather than surface affinity. For example, tip-enhanced Raman scattering (TERS) technique introduces an enhanced electromagnetic field by bringing a nanotip into the vicinity of target molecules. Although TERS provides diffraction-unlimited spatial resolution similar to that from an atomic force microscope, it is time-consuming for large area imaging.<sup>6</sup> Li et al. developed shell-isolated nanoparticle-enhanced Raman spectroscopy, in which SERS-active nanoparticles are coated over the surface with target molecules via wet processes.<sup>7</sup> Lee et al. demonstrated using gold nanorod-loaded filter paper for SERS measurement by prewetting and swabbing it on the surface to be probed.<sup>8</sup>

Our goal is to develop a dry physical approach with decent sensitivity and imaging uniformity. To produce volumetric SERS effects, our group has developed nanoporous gold disks (NPGDs) with large specific areas for effective photothermal conversion<sup>9</sup> and high-density plasmonic hot spots with an average SERS enhancement factor exceeding  $10^8$ , which would provide a promising platform to meet the needs.<sup>10</sup> Herein, we utilize a polydimethylsiloxane (PDMS) thin film as a carrier of target molecules for its low cost, ease of fabrication, mechanical flexibility, biocompatibility, relatively few Raman peaks in the fingerprint region, and low auto-fluorescence. Target molecules are first deposited on the PDMS film, dried, and then stamped onto an NPGD SERS substrate, followed by SERS measurement from “sandwiched” molecules.

## 2 Results and Discussion

Figures 1(a)–1(c) illustrate the S-SERS scheme with the corresponding visual images shown in Figs. 1(d)–1(f). First, 4  $\mu\text{L}$  of the prepared solution containing target molecules was dropped on the PDMS (Sylgard 184, Dow Corning, Midland, Michigan) thin film having a thickness of  $\sim 125 \mu\text{m}$  and a dimension of  $\sim 1 \times 1 \text{ cm}^2$  [see Figs. 1(a) and 1(d)], which was prepared following standard protocols. The droplet was then dried on the PDMS substrate, forming an ultra-thin film of target molecules on the PDMS surface after solvent evaporation in around 30 min [see Figs. 1(b) and 1(e)]. Finally, an NPGD substrate was

\*Address all correspondence to: Wei-Chuan Shih, E-mail: [wshih@uh.edu](mailto:wshih@uh.edu)

<sup>†</sup>These authors contributed equally to this work.

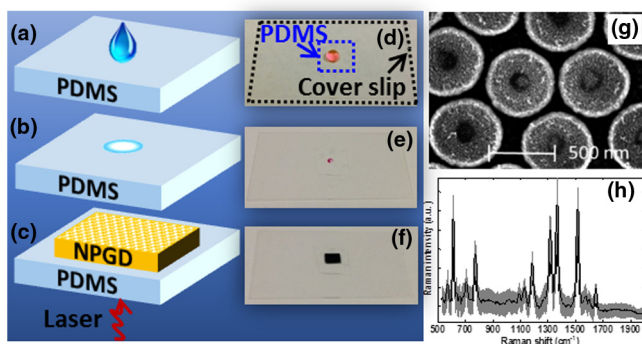


**Fig. 1** Schematics and corresponding images of S-SERS and NPGDs: (a)–(f) See text for details; (g) scanning electron microscopy image of NPGDs; (h) SERS along the laser line from 100  $\mu\text{M}$  Rhodamine 6G (R6G) with average spectrum (black solid line) and  $\pm 1$  standard deviation (gray shade).

stamped onto the PDMS surface with dried molecules, followed by focusing laser at the PDMS surface to detect SERS signals of sandwiched molecules [see Figs. 1(c) and 1(f)]. Monolayer NPGDs densely distributed on Au-coated silicon substrates were fabricated by nanosphere lithography technique as described in our previous work.<sup>10</sup> A scanning electron microscopy image was acquired to show the structure of the NPGDs [see Fig. 1(g)] before stamping.

A home-built line-scan Raman microscopy system with 785-nm excitation laser was employed.<sup>11,12</sup> The laser power on the sample was  $\sim 28$  mW over a  $1 \times 133 \mu\text{m}^2$  line-shaped area, and all the samples were measured with an integration time of 10 to 20 s for each scan step. To verify the performance of the proposed technique, Rhodamine 6G (R6G) with well-characterized SERS spectrum was used. A 4  $\mu\text{L}$  droplet of 100  $\mu\text{M}$  R6G was dropped and dried on the PDMS surface, resulting in a  $\sim 1$  mm spot. First, we examined the measurement uniformity by imaging a region around the midpoint between the center and circumference of the dried spot, which appeared visually uniform under bright-field microscopy. Figure 1(h) shows the statistics of a total of 350 SERS spectra across the laser line where the solid line represents the average spectrum while the gray shade represents  $\pm 1$  standard deviation. The results suggest the decent SERS uniformity across the sampled region.

Next, we show that S-SERS can reveal apparently invisible molecular coatings on PDMS. As shown in Fig. 2(a), R6G Raman spectrum from dried 100  $\mu\text{M}$  solutions on PDMS surface was measured and marked as “Normal.” No normal Raman spectrum was observed from any samples with lower concentrations. NPGD substrate was then gently stamped against the PDMS, after which the sample was measured again and marked as “Stamped.” Major Raman peaks for R6G at 611, 771, 1185, 1317, 1366, 1515, and 1650  $\text{cm}^{-1}$  were observed. The 1366  $\text{cm}^{-1}$  peak intensity for 100  $\mu\text{M}$  R6G exhibits a  $\sim 10$ -fold enhancement after stamping.

To examine the capability of the stamping protocol for potential point-of-care and forensics applications, urea solutions with different concentrations ranging from 10 nM to 100  $\mu\text{M}$  were used to simulate urine tests. The same sample preparation and measurement procedures aforementioned were applied. As shown in Fig. 2(b), excellent intensity enhancement can be seen after stamping, with the primary Raman peak near 1001  $\text{cm}^{-1}$  corresponding to the symmetrical C–N stretching

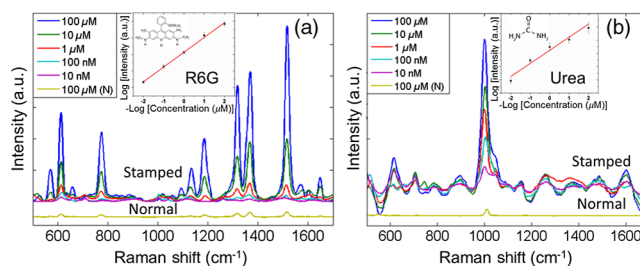


**Fig. 2** Before (“Normal”) and after stamping (“Stamped”) SERS for: (a) R6G and (b) urea. Insets show (a) R6G peak intensity at 1366  $\text{cm}^{-1}$  and (b) urea peak intensity at 1001  $\text{cm}^{-1}$  versus concentrations.

vibration mode clearly observed. We note that the detection limit in the nanomolar range is significantly lower than most SERS results reported in the literature in the millimolar range,<sup>13</sup> although direct comparison is not suggested because our technique employed dried samples as opposed to continuous-flow measurements in microfluidic configurations.

Conventional SERS measurements by transferring molecules of interest to SERS-active substrates can result in the unavoidable loss of spatial distribution of molecules on the original surface. To further demonstrate that the S-SERS technique has the capability to obtain spatio-chemical information from the PDMS surface, we have recorded a three-dimensional (3-D) ( $x, y, \lambda$ ) SERS map from dried 100  $\mu\text{M}$  R6G samples. The SERS map generated by peak intensity at 1366  $\text{cm}^{-1}$  [Fig. 3(b)] showed an identical yet clearer boundary of dried R6G droplet compared with the bright-field image [Fig. 3(a)]. Five different points inside the droplet were chosen and the corresponding spectra were shown in Fig. 3(c).

To demonstrate multiplexed sensing and imaging capabilities, we have recorded a 3-D ( $x, y, \lambda$ ) SERS map from dried mixture samples of 100  $\mu\text{M}$  urea and 1 mM acetaminophen (APAP). These concentrations are relevant for successful detection in urine.<sup>13,14</sup> After stamping, we could not find the dry mark using bright-field microscopy because both molecules are colorless, however, SERS maps successfully provided the spatial distribution information of both. As shown in the bottom row of Fig. 3, the SERS map generated by peak intensity at 1001  $\text{cm}^{-1}$  for urea [Fig. 3(d)] showed a similar overall boundary of the dried droplet to the one generated by a peak intensity at 856  $\text{cm}^{-1}$  for APAP [Fig. 3(e)], but a different spatial distribution. As shown in Fig. 3(f), spectra from five different positions were presented. For example, the peak intensity ratio of urea’s major peak at 1001  $\text{cm}^{-1}$  to that of APAP at 856  $\text{cm}^{-1}$  is 2.45 at position 2, while the ratio is 0.67 at position 4. The results suggest that the two different molecules did not uniformly distribute on the PDMS surface during drying, likely due to differences in density, solubility, concentration, and affinity to the PDMS surface, etc. We note that the mixture data were collected from the circumference to emphasize the detection of the drying edge, where the well known “coffee ring” effect caused more molecular accumulation.

The proposed technique suggests new SERS applications. For example, PDMS is employed as a sample collector in solid-phase microextraction, while our results establish the feasibility for direct molecular analysis on PDMS without additional the sample transfer required in current practice using gas chromatography. A second example is fingerprint sampling using PDMS for forensics, where our approach can provide chemical imaging of the latent fingerprint with associated

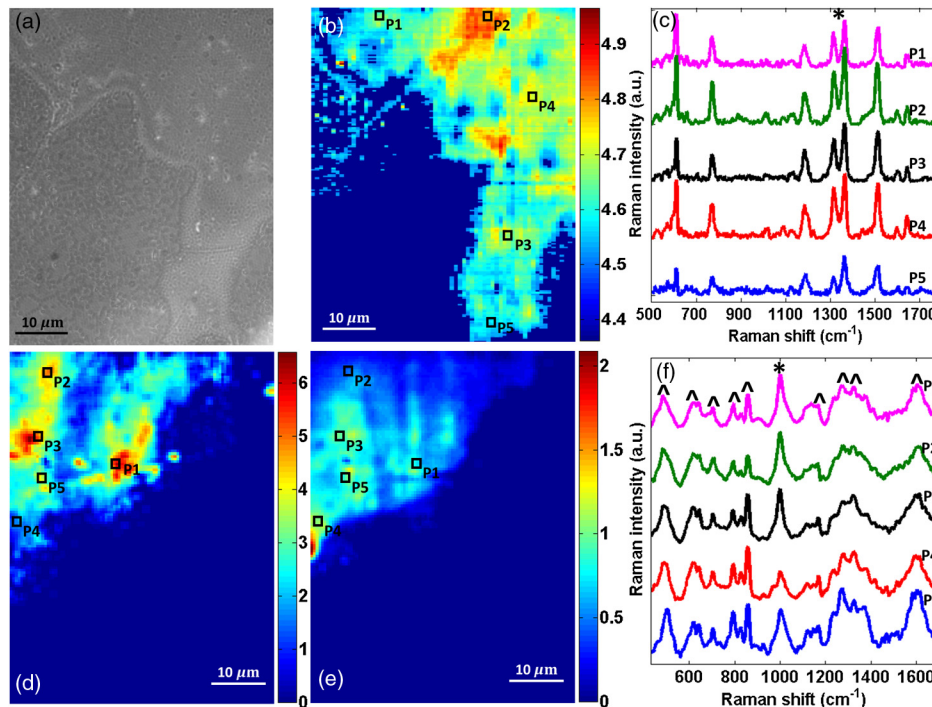


**Fig. 3** SERS image of dried 100  $\mu\text{M}$  R6G (top) and 100  $\mu\text{M}$  urea and 1 mM APAP mixture (bottom): (a) bright field image, (b) SERS map of peak intensity at 1366  $\text{cm}^{-1}$  for R6G, and (c) spectra obtained at five different positions shown in (b). The 1366  $\text{cm}^{-1}$  peak is marked by asterisk. (d) SERS map of peak intensity at 1001  $\text{cm}^{-1}$  for urea, (e) SERS map of peak intensity at 856  $\text{cm}^{-1}$  for APAP, and (f) spectra obtained at five different positions shown in (d) and (e). Major peaks for urea (\*) and APAP (^) are marked.

exogenous molecules. Furthermore, our technique can provide label-free, multiplexed assay of biological fluids such as urine.

### 3 Conclusions

In conclusion, we present a technique called S-SERS for label-free, multiplexed, molecular sensing and imaging in a simple and cost-effective fashion. This technique takes advantage of PDMS as a carrier for target molecules and NPGD with high-density hot spots as the Raman signal enhancer, enabling SERS measurement of sandwiched target molecules without solution-phase sample transfer onto the SERS-active surface. R6G and urea detection with concentrations ranging from 10 nM to 100  $\mu\text{M}$  has been demonstrated. Moreover, large-area, high-resolution SERS maps of multiple molecules dried on the PDMS surface has been demonstrated. By coupling with high-throughput Raman imaging systems based on line-scan or active-illumination,<sup>11,15</sup> this technique can become a powerful tool for forensics analysis. The capabilities of detecting and imaging physiological concentrations of urea and APAP mixtures could lead to new point-of-care applications.

### References

- C. L. Haynes, A. D. McFarland, and R. P. Van Duyne, "Surface-enhanced Raman spectroscopy," *Anal. Chem.* **77**(17), 338A–346A (2005).
- P. D. O'Neal et al., "Feasibility study using surface-enhanced Raman spectroscopy for the quantitative detection of excitatory amino acids," *J. Biomed. Opt.* **8**(2), 33–39 (2003).
- X. B. Xu et al., "Guided-mode-resonance-coupled plasmonic-active SiO<sub>2</sub> nanotubes for surface enhanced Raman spectroscopy," *Appl. Phys. Lett.* **100** (2012).
- C. Ruan, W. Wang, and B. Gu, "Surface-enhanced Raman scattering for perchlorate detection using cystamine-modified gold nanoparticles," *Anal. Chim. Acta* **567**(1), 114–120 (2006).
- S. S. R. Dasary et al., "Gold nanoparticle based label-free SERS probe for ultrasensitive and selective detection of trinitrotoluene," *J. Am. Chem. Soc.* **131**(38), 13806–13812 (2009).
- D. Richards et al., "Tip-enhanced Raman microscopy: practicalities and limitations," *J. Raman Spectrosc.* **34**(9), 663–667 (2003).
- J. F. Li et al., "Shell-isolated nanoparticle-enhanced Raman spectroscopy," *Nature* **464**, 392–395 (2010).
- C. H. Lee, L. Tian, and S. Singamaneni, "Paper-based SERS swab for rapid trace detection on real-world surfaces," *ACS Appl. Mater. Interfaces* **2**(12), 3429–3435 (2010).
- G. M. Santos et al., "Characterization of nanoporous gold disks for photothermal light harvesting and light-gated molecular release," *Nanoscale*, accepted manuscript (2014).
- J. Qi et al., "Surface-enhanced Raman spectroscopy with monolithic nanoporous gold disk substrates," *Nanoscale* **5**(10), 4105–4109 (2013).
- J. Qi and W.-C. Shih, "Parallel Raman microspectroscopy using programmable multipoint illumination," *Opt. Lett.* **37**(8), 1289–1291 (2012).
- J. Qi and W.-C. Shih, "Performance of line-scan Raman microscopy (LSRM) for high-throughput chemical imaging of cell population," *Appl. Opt.* **53**(13), 2881–2885 (2014).
- H.-Y. Wu, C. J. Choi, and B. T. Cunningham, "Plasmonic nanogap-enhanced Raman scattering using a resonant nanodome array," *Small* **8**(18), 2878–2885 (2012).
- M. Sanaka et al., "Use of salivary acetaminophen concentration to assess gastric emptying rate of liquids," *J. Gastroenterol.* **35**(6), 429–433 (2000).
- J. Qi, J. Li, and W.-C. Shih, "High-speed hyperspectral Raman imaging for label-free compositional microanalysis," *Biomed. Opt. Express* **4** (11), 2376–2382 (2013).